Nuclear Instruments and Methods in Physics Research A 620 (2010) 67–70

Contents lists available at ScienceDirect

Nuclear Instruments and Methods in Physics Research A

journal homepage: www.elsevier.com/locate/nima

# Ultrafast $CO_2$ laser technology: Application in ion acceleration

I.V. Pogorelsky [a,*], V. Yakimenko [a], M. Polyanskiy [a], P. Shkolnikov [b], M. Ispiryan [b], D. Neely [c], P. McKenna [d], D. Carroll [d], Z. Najmudin [e], L. Willingale [e,f]

[a] ATF, Brookhaven National Laboratory, Upton, NY 11973-5000, USA
[b] Department of Electrical and Computer Engineering, SUNY at Stony Brook, NY 11794-2350 , USA
[c] Central Laser Facility, Rutherford-Appleton Laboratory, Chilton, Oxon, OX11 0QX, UK
[d] SUPA Department of Physics, University of Strathclyde, Glasgow G4 0NG, UK
[e] Blackett Laboratory, Imperial College London, London SW7 2BZ, UK
[f] Center for Ultrafast Optical Science, University of Michigan, Ann Arbor, Michigan, 48105, USA

ARTICLE INFO

Available online 1 February 2010

*Keywords:*
$CO_2$ laser
Protons
Ion acceleration

ABSTRACT

We review principles of picosecond $CO_2$ lasers, operating at 10 μm wavelength, and their applications for strong-field physics research. Such laser has been used in a number of BNL experiments that explore advanced methods of particle acceleration and X-ray generation. We illustrate merits of the wavelength scaling from optical to mid-IR region by the examples of ion/proton acceleration and report the first experimental results that confirm the expected wavelength scaling of the process.

Published by Elsevier B.V.

## 1. Introduction

Mainstream experimental research in strong-field physics capitalizes so far on the chirped pulse amplification (CPA) solid-state lasers that have reached petawatt peak power and $10^{21}$ W/cm$^2$ intensities. Concurrently, there is interest in exploring the capabilities of the $CO_2$ gas lasers. While the peak power of $CO_2$ lasers can hardly compete with that of solid-state lasers, relativistic intensities are already available, and longer wavelength ($\sim$10 μm) may offer significant advantages in applications, as well as a window into new areas of high-intensity laser-matter interactions. Presently, Neptune Laboratory at UCLA and the Accelerator Test Facility (ATF) at BNL conduct strong-field physics experiments with $CO_2$ lasers.

The following summary of the key potential benefits of high-intensity $CO_2$ lasers for R&D on advanced accelerators and radiation sources is based on the ATF's 15-year experience in using long-wavelength laser radiation combined with a 70-MeV high-brightness electron linac.

Our first premise is the ease of scaling of structure-based laser accelerators, and electron phasing into the laser field, as illustrated by STELLA, the first staged monoenergetic laser accelerator founded on the principle of the inverse free electron laser (IFEL) [1]. In STELLA, the laser and electron beams co-propagate through two successive wigglers. In the first wiggler (the "buncher"), the laser provides periodical energy modulation of the electron beam, which subsequently divides into femtosecond microbunches at the location of the second wiggler ("accelerator"). Being periodically spaced exactly to the laser's wavelength, the microbunches in the accelerator experience a uniform acceleration when phased to the laser's field maximum amplitude, as has been demonstrated in our experiment. Such wavelength-accuracy is difficult to achieve with the much shorter-wavelength optical radiation of CPA lasers.

Other applications gain from the proportionally larger number of photons per joule of laser energy at longer wavelength. For example, a higher X-ray yield in inverse Compton scattering is achieved from counter-propagating the electron- and $CO_2$ laser-beams [2]. This demonstration strongly argues for the excellent prospects of ultra-bright laser synchrotron sources for multi-disciplinary applications [3].

At the center of our research reported here is another favorable wavelength scaling, that of the electron ponderomotive potential in a laser field:

$$\Phi_{pond} = \frac{1}{4}\frac{e}{m\omega_L^2}|\vec{E}_0|^2.$$

It ensures that relativistic quiver motion $\Phi_{pond}=mc^2$ is reached at a hundred times lower laser intensity at 10 μm than at 1 μm. (This relativistic condition is usually expressed as $a_0=1$ via dimensionless laser strength $a_0 = 0.89\sqrt{I_{18}}\lambda$, where $I_{18}$ is the laser beam's intensity in units of $10^{18}$ Wcm$^{-2}$ and $\lambda$ in μm.) The favorable wavelength scaling was a factor that enabled our direct single-shot imaging of the second harmonic in inverse Compton scattering [4]. As the collective ion motion in laser fields is usually driven by ponderomotively accelerated plasma electrons, we expect this scaling to benefit laser-driven ion acceleration.

* Corresponding author.
*E-mail address:* igor@bnl.gov (I.V. Pogorelsky).

0168-9002/$ - see front matter Published by Elsevier B.V.
doi:10.1016/j.nima.2010.01.062

In particular, the main mechanism responsible for the observed laser acceleration of protons and ions by lasers interacting with thin foils, TNSA, relies on relativistic electrons accelerated by the laser [5].

Since our laser is inherently circularly polarized, proton acceleration in our experiments may occur also by another mechanism, Radiation Pressure Acceleration (RPA) [6]. A simplified theoretical model for RPA yields the maximum proton energy and accelerated photon number at

$$E^p_{\max}(MeV) \approx (n_c/n_e)a_0^2, \quad N \approx Sn_{i0}\lambda/4\pi, \tag{1}$$

where $n_e$ is the electron density in the area where the acceleration takes place; $n_c=\pi/(r_e\lambda^2)$ is the critical electron density; $r_e \approx 2.8 \times 10^{-13}$ cm is the classical electron radius, $S$ is the laser focus spot area, and $n_{i0}$ is the ion density in this area.

Assuming that the deposition of laser energy and ion acceleration mainly occur near the critical plasma density, $n_e \approx n_{i0} \approx n_c$, Eqs. (1) are simplified to

$$E^p_{\max}(\mathrm{MeV}) \approx a_0^2, \quad N^p \sim \lambda/r_e. \tag{2}$$

Thus, both $E^p_{\max}$ and $N^p$ scale favorably with $\lambda$. A similarly simple wavelength scaling can be derived for TNSA mechanism with the difference of $E^p_{\max}(\mathrm{MeV}) \propto a_0$ [5].

Another factor to consider is the hundredfold lowering of the critical plasma density when changing the laser's wavelength from 1 to 10 μm.

Overall, little experimental evidence has been accumulated so far regarding high-intensity, ultrafast laser-plasma interaction at longer laser wavelengths to confirm theoretical wavelength scaling. In view of that, we began exploring proton/ion acceleration by the ATF $CO_2$ laser in collaborative effort that includes: SUNY at Stony Brook, USA; Rutherford Appleton Laboratory, UK; University of Strathclyde, UK; Imperial College, UK; and BNL, USA.

## 2. Experiment

The ion acceleration experiment has required a number of modifications in the BNL $CO_2$ laser operations. First of all, the efficiency of laser radiation in terms of producing intense ion beams depends significantly upon the laser's contrast factor, because a pre-pulse produces a shock wave in the foil target that melts and blurs the sharp solid-vacuum interface at the rear surface of the target, which is essential for TNSA. The pre-pulse control was not vital for our earlier ATF experiments wherein the laser was used primarily for interacting with the e-beam in a vacuum (e.g., for electron acceleration, or inverse Compton scattering). Therefore, at the initial stage of our ion-acceleration experiment, we made considerable effort to bring the laser to the acceptably high contrast level. This included blocking the picosecond pre-pulses, emerging due to power circulation in a regenerative amplifier cavity, from their leakage from the cavity and further amplification in the final amplifier. We accomplished this using a Pockels cell switch between crossed polarizers, so ensuring a power contrast at $10^4$ between the main pulse and a picosecond pre-pulse that precedes the main pulse by 30 ns (round trip time in the regenerative amplifier cavity). No detectable ASE pedestal as well as no pre-plasma at the target's surface have been observed.

Another fundamental problem arises from the erosion of the spectral envelope of a picosecond $CO_2$ laser by the rotational structure of molecular spectrum in the amplifier. Simulations as well as optical diagnostics revealed that the Fourier transform of such a spectrum results in a train of pulses (see Fig. 1). These same tools guided us to switch from the conventional P-branch of the $CO_2$ laser spectrum to the R-branch. In the future, we will change to using a multi-isotope mixture that ensures single-pulse amplification. Meantime, partial pulse-splitting, as is shown in Fig. 1 (7.5 atm, R-branch), remains a factor that may influence our results.

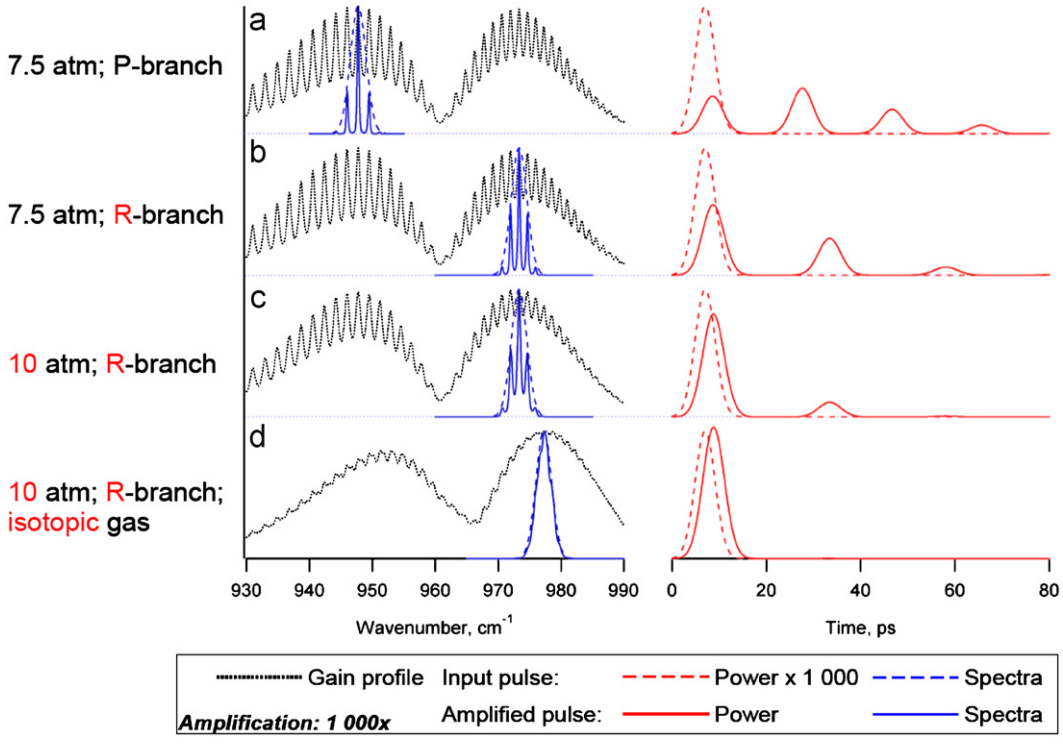


**Fig. 1.** Simulated spectral- and temporal-modulation of a 5-ps Gaussian $CO_2$ laser pulse during 1000-times energy amplification.